Plant Mol Biol (2007) 63:237–255
DOI 10.1007/s11103-006-9085-z

Arabidopsis immunophilins ROF1 (AtFKBP62) and ROF2 (AtFKBP65) exhibit tissue specificity, are heat-stress induced, and bind HSP90

Keren Aviezer-Hagai · Julia Skovorodnikova · Mario Galigniana · Odelia Farchi-Pisanty · Erez Maayan · Shmuel Bocovza · Yael Efrat · Pascal von Koskull-Döring · Nir Ohad · Adina Breiman

Received: 4 June 2006 / Accepted: 30 August 2006 / Published online: 2 November 2006

Abstract The plant co-chaperones FK506-binding proteins (FKBPs) are peptidyl prolyl *cis-trans* isomerases that function in protein folding, signal transduction and chaperone activity. We report the characterization of the *Arabidopsis* large FKBPs ROF1 (AtFKBP62) and ROF2 (AtFKBP65) expression and protein accumulation patterns. Transgenic plants expressing ROF1 promoter fused to GUS reporter gene reveal that ROF1 expression is organ specific. High expression was observed in the vascular elements of roots, in hydathodes and trichomes of leaves and in stigma, sepals, and anthers. The tissue specificity and temporal expression of ROF1 and ROF2 show that they are developmentally regulated. Although ROF1 and ROF2 share 85% identity, their expression in response to heat stress is differentially regulated. Both genes are induced in plants exposed to 37 °C, but only ROF2 is a bonafide heat-stress protein, undetected when plants are grown at 22 °C. ROF1/ROF2 proteins accumulate at 37 °C, remain stable for at least 4 h upon recovery at 22 °C, whereas, their mRNA level is reduced after 1 h at 22 °C. By protein interaction assays, it was demonstrated, that ROF1 is a novel partner of HSP90. The five amino acids identified as essential for recognition and interaction between the mammalian chaperones and HSP90 are conserved in the plant ROF1-HSP90. We suggest that ROF/HSP90 complexes assemble in vivo. We propose that specific complexes formation between an HSP90 and ROF isoforms depends on their spatial and temporal expression. Such complexes might be regulated by environmental conditions such as heat stress or internal cues such as different hormones.

Keywords ROF1/2 · AtFKBP62/65 · Immunophilins · HSP90 · TPR · PPIase

Abbreviations

FKBP	FK506-binding protein
PPIase	Peptidyl prolyl *cis-trans* isomerase
Cyp40	Cyclophilin 40
CsA	Cyclosporin A
TPR	Tripartite tetratricopeptide repeats
HOP	HSP70 and HSP90 organizing protein
FKBD	FKBP12-like domain
CaMBD	Calmodulin binding domain
GUS	β-Glucoronidase
HSP	Heat shock protein
PP5	Protein phosphatase 5
HSF	Heat shock factor
HSE	Heat shock element
STRE	Stress response element

Electronic supplementary material Supplementary material is available in the online version of this article at http://dx.doi.org/10.1007/s11103-006-9085-z and is accessible for authorized users.

K. Aviezer-Hagai · J. Skovorodnikova · O. Farchi-Pisanty · E. Maayan · S. Bocovza · Y. Efrat · N. Ohad · A. Breiman (✉)
Department of Plant Sciences, Tel Aviv University, Tel Aviv, Israel
e-mail: adina@post.tau.ac.il

M. Galigniana
Instituto de Investigaciones Bioquimicas, Fundacion Instituto Leloir Buenos Aires, Buenos Aires, Argentina

P. von Koskull-Döring
Institute of Molecular Bio Sciences, Goethe University, Frankfurt, Germany

Introduction

The FK506-binding proteins (FKBPs) belong to the superfamily of peptidyl prolyl *cis-trans* isomerases (PPIases) (EC 5.2.1.8), which are present in all organisms and almost all subcellular compartments (Galat 2004; Romano et al. 2005). The catalytic activity of PPIase is the rotation of a peptide bond preceding proline in the proteins (Fischer et al. 1998; Fanghanel and Fischer 2004). The FKBPs are a distinct set of cellular receptors, which bind the immunosuppressive-drugs FK506 and rapamycin. When FKBPs bind these drugs their PPIase activity is inhibited (Schreiber 1991). The complexes formed by the FKBPs and their ligends are the functional modules for immunosuppression. Based on this activity, the FKBPs, together with the unrelated family of cyclophilins (CyPs) [which bind the immunosuppressive drug cyclosporine A (CsA)] have also been termed immunophilins. The drugs FK506 and CsA are involved in the mechanism of immunosuppression, and therefore the immunophilins are extensively studied as reviewed (Galat 2003, 2004; Dornan et al. 2003; He et al. 2004; Romano et al. 2005).

During the past decade, a growing number of immunophilins from mammalian, bacteria, and plants have been characterized. The high-level of conservation among the FKBP-protein family and ubiquitous distribution suggest that they participate in important cellular processes. However, only in few cases the cellular function of FKBPs has been elucidated (He et al. 2004; Romano et al. 2005).

The FKBP family consists of multiple members that are distinguished by molecular weight ranging from 12 kDa (hFKBP12, AtFKBP12) (Standaert et al. 1990; Faure et al. 1998a) to over 77 kDa (wFKBP77) (Kurek et al. 1999). They are found in almost all subcellular locations including endoplasmic reticulum (Luan et al. 1996; Zhang et al. 2004), chloroplast (Luan et al. 1994), cytosol (Standaert et al. 1990; Dwivedi et al. 2003), nucleus (Jin et al. 1992), and mitochondria (Breiman et al. 1992).

The human FKBP12, which comprises of a single FKBP domain, is the gene that provides the common denominator for the family. The proteins possessing sequence homology to this domain have been designated members of the FKBP family with FKBP12-like domains.

Multidomain FKBPs are structurally characterized by additional protein modules, typically a tripartite tetratricopeptide repeats (TPR) domain, which is involved in protein–protein interaction (Goebl and Yanagida 1991) and a calmodulin-binding domain (CaMBD) (He et al. 2004). In the large FKBPs studied, the first FKBP12-like domain exhibits PPIases activity in vitro (Chambraud et al. 1993; Blecher et al. 1996). The large FKBP group is exemplified by the mammalian FKBP52, which is the major immunophilin of the multiprotein glucocorticoid receptor complex (Smith et al. 1993).

In plants, high-molecular weight FKBP members have been identified from wheat (Blecher et al. 1996; Kurek et al. 1999), *Arabidopsis* (Vucich and Gasser 1996; Vittorioso et al. 1998; Geisler et al. 2004; Perez-Perez et al. 2004), maize (Hueros et al. 1998), and recently also from rice (Magiri et al. 2006).

The completion of the *Arabidopsis* genome sequencing revealed 23 FKBP members, being one of the largest FKBP families identified. The *Arabidopsis* FKBPs can be classified into those bearing single-or multiple-domains, among which seven members contain multiple domains (He et al. 2004; Romano et al. 2005).

The role of two *Arabidopsis* large FKBPs has been recently explored. The *PASTICCINO1* (*PAS1*) protein is a member of the large FKBP-family and the mutants, impaired in the AtFKBP72 coding region, display severe developmental abnormalities throughout the growth stages, altered response to cytokinins and down-regulation of primary auxin responsive genes, suggesting that this protein play a role in cytokinin and auxin response (Vittorioso et al. 1998; Harrar et al. 2003). The characterization of the twisted dwarf1 (twd1) (Geisler et al. 2003) and ultracurvata 2 (UCU2) (Perez-Perez et al. 2004) both knockouts of At FKBP42, revealed common pleiotropic effects leading to dwarfism, distorted roots, and stems as well as helical rotation of organs. The AtFKBP42 protein was shown to interact with ABC transporters, and when mutated, vacuolar transport is affected (Geisler et al. 2003, 2004). In addition TWD1 was shown to bind HSP90 (Kamphausen et al. 2002). Recently, the crystal structure of the AtFKBP42 was solved (Eckhoff et al. 2005; Weiergraber et al. 2006). The function of the other, structurally different, plant large FKBPs in the cell requires further investigation.

Among the large FKBPs, which have been identified in plants, the expression of the wheat wFKBP77 (Kurek et al. 1999) and rice rFKBP65 (Magiri et al. 2006) genes were shown to be elevated by heat stress. The *Arabidopsis* ROF1 gene expression was found to be increased by wounding or exposure to elevated NaCl levels (Vucich and Gasser 1996).

High molecular-weight immunophilins from mammals (FKBP51, FKBP52, and CyP40) have been identified by their abilities to bind HSP90 via TPR-domains, as components of unliganded steroid receptor heterocomplexes. This interaction occurs

through the heat shock protein 90 (HSP90) (Sanchez et al. 1990; Pratt et al. 2004). HSP90 is a highly abundant cytosolic protein, which is important under both stress and physiological conditions. It acts as the central platform for distinct multichaperone complexes as the steroid receptor complex, with additional cofactors, including p23 (Pirkl and Buchner 2001; Riggs et al. 2003).

The crystal structures of the TPR-containing immunophilins: CyP40 (Ward et al. 2002), FKBP51 (Sinars et al. 2003) and FKBP52 (Wu et al. 2003, 2004) in complex with a peptide containing the C-terminal residues of HSP90 (MEEVD motif) enabled the identification of the five residues of the TPR, essential for HSP90 binding. These five key residues were also found to be conserved in the TPR-containing chaperones HOP (HSP70 and HSP90 organizing protein, also known as p60 or Sti1p) (Scheufler et al. 2000; Carrigan et al. 2006) and in protein phosphatase 5 (PP5) (Das et al. 1998). Recent experiments in plants have suggested that the multiprotein complex components of this chaperoning machinery are likely to be conserved between animal and plant kingdoms (Owens-Grillo et al. 1996; Reddy et al. 1998; Harrell et al. 2002).

From studies of the mammalian and plants FKBPs it appears that the common denominator of this protein family, namely the FKBP12-like domain, represents an evolutionary conserved domain relevant to taxonomic resemblance (Galat 2004). However, each member has gained an unique function in context to its intracellular localization and protein client (Geisler et al. 2004, Davies et al. 2005).

The FKBP superfamily contains pairs of proteins that share a high-sequence identity but were shown to have different functions. Such is the case for the mammalian homologues FKBP51 and FKBP52, which share high-sequence similarity, but associate with different steroid receptors (Davies et al. 2005). In plants, the wheat FKBP73 and FKBP77 were shown to be cognate and heat-stress induced counterparts (Kurek et al. 1999). The *Arabidopsis* large FKBPs, AtFKBP62 (ROF1), and AtFKBP65 (ROF2) share similar domain structure and high sequence identity.

In order to gain better understanding for the role of the two homologues, the *Arabidopsis* ROF1 and ROF2 have been characterized. A detailed glucuronidase (GUS) histochemical analysis of ROF1 promoter at various stages of plant development, revealed specific vascular staining pattern in young and mature vegetative tissues and in reproductive organs. Differential expression between the two ROF genes at RNA and protein levels was displayed. Furthermore, we show that the *Arabidopsis* ROF1 can specifically bind HSP90.

Materials and methods

Plant material

Arabidopsis thaliana plants ecotype columbia (Col-0) were used for ROF1 and ROF2 promoter analysis, and ecotype wassilewskija (WS) for creation of *rof1* and *rof2* mutants and for RNA and protein expression analysis. Plants were grown at long-day conditions (16 h light, 8 h dark) at 22 °C, unless differently mentioned.

Analysis of ROF1 and ROF2 expression in vivo was performed by β-glucuronidase assays. We have constructed transgenic plants bearing fusion between the ROF1 or ROF2 promoter and the *uidA* gene. The promoter sequences were cloned by amplification from MJL12 cosmid containing chromosome 3 (Table 1) and ROF2 putative promoter from *Arabidopsis* genomic DNA. The polymerase chain reaction (PCR) amplification was carried out using the primers anchoring the region upstream the ATG start codon and reaching the stop codon of the previous gene located 1,848 and 629 bp upstream to ROF1 and ROF2, respectivly (ROF1/2 promoter F and R) (Table 2). The putative promoter fragments were fused to GUS reporter gene (*uidA* gene) by *Xho*I–*Nco*I sites in WRG2920 plasmid (Table 1). After verification by sequencing, these constructs containing the nopaline synthatse gene were sub-cloned into pCAMBIA 1,300 binary vector (Table 1). Next, these vectors were transformed into *Arabidopsis* plants via the floral dip method (Clough and Bent 1998) using *Agrobacterium tumefaciens* GV3101 (Bechtold et al. 1993). Approximately 100 sterilized T1 seeds from each T0 transformed plant were germinated on MS-agar containing hygromycin (60 (μg/ml) plates. The selected plantlets were then transferred to soil and grown to yield T2 seeds. Four homozygous T2 lines containing ROF1::GUS (ROF1.4.1, ROF1.5.1, ROF1.7.1, and ROF1.10.1) lines and 4 ROF2::GUS (ROF2.2.1, ROF2.8.1, ROF2.10.1, and ROF2.15.1) lines were selected for further analysis by PCR, southern analysis and GUS expression assays.

Genomic DNA from transgenic plants (shoots) was isolated by the method described by Clark (1997). PCR was performed to verify the T-DNA insertion by using the primers of ROF1 promoter F or ROF2 promoter F with the GUS primer (Table 2). The pCAMBIA1300 containing the promoter fragments were used as a positive-template DNA. The number of incorporated copies of the GUS gene was analyzed by Southern blot. This was carried out by digesting 4 μg of genomic DNA isolated from the 4 ROF1 and ROF2 transgenic

Table 1 strains, vectors, and cosmids

Name	Selection bacteria/plant	Purpose	Source
MJL12 (*Arabidopsis thaliana* genomic DNA, chromosome 3)		Amplification of ROF1 promoter	AB026647 (NCBI)
pWRG2920	Ampicillin	Cloning ROF1 and ROF2 promoters upstream *β*-GUS gene	Christou and Ford (1995)
pCAMBIA 1300	Kanamycin/ hygromycin	Binary vector for *Arabidopsis* transformation	CAMBIA http://cambia.org.au
pKANNIBAL	Kanamycin	Cloning RNAi constructs for ROF2 silencing	Wesley et al. (2001)
pART27	Spectinomycin/ Kanamycin	Binary vector for cloning NotI fragment from pKANNIBAL	Gleave (1992)
pET28	Kanamycin	Expression vector for ROF1 mutated forms	

T3 lines (expressing the GUS reporter gene) with *Nco*I and *Hin*dIII, respectively. Following enzymatic digestion the DNA was separated using 0.8% agarose gels, transferred onto nylon membrane (Hybond-N^+ Amersham Pharmacia Biotech) according to manufacturer instructions, and hybridized with a fragment of the GUS gene and NOS terminator (*Eco*RV-*Kpn*I from pWRG2920) as a probe. The analysis showed that two ROF1 transgenic lines (ROF1.7.1 and ROF1.10.1) and two ROF2 lines (ROF2.2.1 and ROF2.15.1) contained two copies of the insert while the other lines contained more than two copies except ROF2.8.1 containing one copy. These lines were subjected to GUS expression assays.

For isolation of the *Arabidopsis rof1* knockout mutant, a tagged T-DNA library available in versailles was screened (this work was done in collaboration with Drs. Bellini and Faure in INRA, Versailles, France). The *rof1* knockout mutant was found to contain a T-DNA insertion in its third intron; consequently the protein is not produced.

For isolation of *rof2* mutant we used the SiRNA strategy (Fire et al. 1998). Specific primers according to ROF2 nucleotide sequence were designed (nucleotide

Table 2 Primers used for PCR in this study

Primer name	Primer sequence	Length (bp)	Purpose
ROF1 promoter F	5′CCGCTCGAGGGATTATCAGTCTATCTTTTATTGG 3′	1848	ROF1 promoter amplification
ROF1 promoter R	5′CATGCCATGGTTTTTCGATTCAGTTCCAAAC 3′		
ROF2 promoter F	5′CCGCTCGAGCATAACTATACATAAACTAGTTAGCCAC 3′	629	ROF2 promoter
ROF2 promoter R	5′CATGCCATGGTTTCTGATCAAATTTAAGAGAGTGAA 3′		
GUS	5′CTGATGCTCCATCACTTCCTG 3′		GUS transgenic lines verification by PCR
ROF2 1197–1418 F	5′CGCGGATCCCTCGAGCCACAAGTGATAGAAGGGCTTG 3′	221	ROF2 SiRNA
ROF2 1197–1418 R	5′CCCGAATTCATCGATCGAGCTCTTGCGTATTTTCCAGC 3′		
ROF1 3′UTR F	5′GCGAAACTAAGTAAGGAATAATCA 3’	171	RT-PCR
ROF1 3′UTR R	5′GCAACACATTGGGATAATCTC 3′		
ROF2 3′UTR F	5′GGAAGCACAAGCGATGAGTATTG 3′	158	RT-PCR
ROF2 3′UTR R	5′GATCCTCGTTTATTACAAGTCTG 3′		
β-actin I F	5′GGTAACATTGTGCTCAGTGGTGG 3′	107	RT-PCR
β-actin I R (An et al. 1996)	5′AACGACCTTAATCTTCATGCTGC 3′		
5′ ROF1 F	5′CGCGGATCCATGGATGCTAATTTCGAGATGCCT 3′		ROF1 coding sequence amplification
3′ ROF1 R	5′CGCGGATCCTTATTCCTTACTTAGTTTCGCAAAC 3′		
ROF1 K404A & N408A F	5′GCTGCTAGTAAGAAGGCGGAAGAAGGAGA TTCCAAGTTTAAAGGAGGC 3′		Mutation of Lys 404 to Ala, and Asn 408 to Ala
ROF1 N454D F	5′GGCATGCAATCTAGACGATGCAGCCTGCAAAC 3′		Mutation of Asn 454 to Asp
ROF1 K484A F	5′GAAAGCACCAATGTGGCGGCCTTATACCGGAGAGC 3′		Mutation of lys 484 to Ala
ROF1 R488A F	5′TGGCGGCCTTATACGCGAGAGCGCAAGCGTAC 3′		Mutation of Arg 488 to Ala

1,197–1,418) (Table 2). This region was cloned into pKANNIBAL transient vector (Table 1). A pKANNIBAL *Not*I fragment containing the CaMV35S promoter, the ROF2 regions separated by the intron, and the OCS terminator, was cloned into pART27 (Table 1) for transformation mediated by *Agrobacterium* into *Arabidopsis* plants (as detailed above). Transgenic plantlets were selected on antibiotics and than transferred to soil for three generations. Subsequently, homozygous T3 2-week-old seedlings from eight independent lines were analyzed by Western blot for ROF1 and ROF2 expression. In three independent lines the ROF2 protein was not detected, while in the other lines the ROF2 expression level was reduced. Under normal growth conditions no obvious phenotypes were found, although the ROF1 or ROF2 proteins were not detected by Western blot (Fig. 8A). The generation and characterization of the *rof1/rof2* double mutant is in progress.

Growth and heat-stress conditions

Arabidopsis thaliana plants were grown on soil (as detailed above) for about 30 days. Seedlings were germinated on MS-medium plates (Murashige and Skoog including vitamins, Duchefa) containing 0.2% MS (w/v), 2.5 mM MES, 1% sucrose, and 0.5% plant agar (Duchefa) for 7–14 days. After 2–3 days at 4 °C in the dark for stratification, seeds grown on soil or plates were grown at 22 °C in long-day conditions.

The mature *Arabidopsis* plants and the seedlings were subjected to heat-stress treatments. For histochemical GUS expression analysis, 2-weeks old ROF2–GUS transgenic seedlings were incubated for 3 h at 37 °C. For reverse transcription polymerase chain reaction (RT-PCR) analysis, mature wild-type (WT) plants were exposed to 37 °C for 1 h in an incubator with high humidity to avoid drought stress. Then tissues (open flowers, buds, siliques, stems, cauline leaves, and rosette leaves) were collected and immediately frozen in liquid nitrogen, followed by RNA isolation. For protein analysis 2-week old seedlings were subjected to various temperatures and times (see legends for figures).

Data analysis

To obtain an estimate of the relative levels of ROF1 and ROF2 mRNAs at various tissues and in response to heat treatments, locus IDs were used to query the genevestigator *A. thaliana* microarray database and analysis toolbox (https://www.genevestigator.ethz.ch) (Zimmerman et al. 2004, 2005).

Relevant, public available experiments were chosen from the database. For our analysis, only experiments that have used affymetrix ATH1 chip hybridized with RNA from WT, nontreated, soil-grown plants of Col-O ecotype were chosen. The chosen experiments are indicated in Table 3.

The digital northern tool was used to retrieve signal values of ROF1 (At3g25230), ROF2 (At5g48570), and for the heat stress series also HSP 17.6 class I (At1g59860), in selected set of chips. Data average was carried between chips of different experiments only if the biological material was congruent and the standard deviation value was no greater then 20% of the average value.

Table 3 Chosen experiments used for ROF1 and ROF2 tissue and heat-stress profiles

Tissue	Chip source	Experiment	Experimenter	# of chips
Flower staging	AtGenExpress	Development baseline III	Weigel	12
Silique	AtGenExpress	Seed and silique development	Weigel	9
	NASC	Silique senescence in *Arabidopsis thaliana*	Thomas Yang/ Jerry Roberts	6
Young (green) seed	AtGenExpress	Seed and silique development	Weisshaar	15
Dry seed	AtGenExpress	Gene expression of Col-0 seeds at 0, 1 and 3 h post imbibition	RIKEN, Preston	2
Stem	NASC	Role of COV in vascular patterning	Simon Turner	4
Shoot apex	AtGenExpress	Development baseline II	Weigel	6
Cauline leaf	AtGenExpress	Development baseline II	Weigel	3
Rosette	AtGenExpress	Development baseline II	Weigel	9
	AtGenExpress	Rosette development (phase change)	Poethig	3
Root	AtGenExpress	Root & shoot development	Scheres	12
	AtGenExpress	Plant organs: comparison with CAGE data	CAGE	3
Heat stress[a]	AtGenExpress	Stress treatment—Heat	Nover/von Koskull-Döring	32

[a] For the heat-series 16-day-old seedlings were used

Signal intensity value below 200 means no or very-low expression, signal intensity value between 200 and 800 means the noise area where results are ambiguous, and signal intensity value higher than 1,000 means expression.

Sequences alignment was carried out using ClustalW (http://www.ebi.ac.uk/clustalw/) and BoxShade (http://www.ch.embnet.org/software/BOX_form.html) softwares.

The Swiss pdb program (www.expasy.org) was used for the modeling of ROF1 TPR domain-structure based on HOP crystal structure, together with its bound HSP90-peptide (HSP90-MEEVD) (Scheufler et al. 2000). The mutational analysis of the HSP90 interacting domain of Cyp40 (Ward et al. 2002) was used to produce mutated ROF1 in order to identify the amino acids that contribute to the HSP90 binding.

GUS expression analysis

Histochemical GUS staining

The histochemical localization of GUS in transformed *Arabidopsis* plants was preformed as described by Jefferson (1987). *Arabidopsis* seedlings or tissues (roots and different stages of leaves, flowers, and siliques) expressing ROF1 or ROF2 promoter–GUS fusion were freshly collected and immersed in a histochemical reaction mixture containing 1.1 mM X-Gluc (5-bromo-4-chloro-3-indolyl-β-D-Glucuronide; Duchefa) in 100 mM potassium phosphate buffer pH 7.0, 5 mM potassium ferrocyanide, 5 mM potassium ferricyanide and 0.1% Triton X-100. Plant material was vacuum infiltrated from 5 min (seedlings) to 15 min (mature tissues). The histochemical reaction was preformed in the dark at 37 °C for 20–360 min. Stained seedlings and tissues were incubated in a clearing solution (2-chloral hydrate: 1-lactic acid v/v) for up to 2 weeks and then placed in a 90% lactic acid medium on a slide and examined with a stereomicroscope (Zeiss SV11) and documented by a Nikon coolpix camera.

Histological sections and microscopy

For localization of GUS expression in various stages of flower development (Smyth et al. 1990; Bowman 1994) the stained tissues were cleared in 70% ethanol overnight, fixed in FAA solution (50% ethanol, 5% acetic acid, and 3.7% formaldehyde) and dehydrated using the tertiary butyl alcohol method. The plant material was embedded in paraffin and cut into 8–12 μm cross thick sections using Microtome 820 (Spencer). After removing the paraffin by solvent, the sections were mounted in glycerol and examined by light microscopy. For analysis of GUS expression in transverse sections of transgenic roots, 2-week old stained tissue were washed with water and cut into 1–1.5 cm long sections. The sections were dipped in petri dish containing 3% agar (in parallel to the agar surface). Pieces of agar containing the root sections were taken out and cut into 60–80 μm sections in ice water surrounding using cold vibrotome Leica VT1000S (Leica, Germany). The histochemical sections were observed using Zeiss Axioplan2 microscope and documented using a Nikon digital camera as indicated above.

RNA isolation and reverse transcription polymerase chain reaction analysis

Total RNA was isolated from various tissues (50–100 mg) before and after heat-stress treatment using SV total RNA Isolation Kit (Promega, USA) according to the manufacturer's instructions. All RNA samples were quantified spectrophotometrically at 260 nm using a nano drop-ND-1000 spectrophotometer (Rockland, DE). First-strand cDNA was produced using 2 μg of total RNA, oligo (dT)15 primer and M-MLV reverse transcriptase (Promega, USA). The resulting cDNA was diluted 10 times and 2 μl were used as a template in 25-μl PCR reaction using gene specific primers designed from the non-homologous regions (3′UTR) of the ROF1 and ROF2 genes (Table 1). The primers were analyzed using Vectors NTI software program. β-actin I was chosen as an internal standard for determining the RT-PCR amplification efficiency among different reactions. PCR amplification was carried out using the following program: 94 °C for 4 min followed by five cycles at 94 °C for 45 s, 55 °C for 45 s and 72 °C for 1 min and then 18 (for β-actin) or 22 cycles (for ROF1 and ROF2) at 94 °C for 30 s, 55 °C for 45 s and 72 °C for 2 min. The reaction was terminated by 72 °C for 5 min. A total of 5 μl of each PCR-product were analyzed by standard 1.5% agarose gel electrophoresis and visualized with ethidium bromide staining. The PCR reactions were performed using the PTC-200-PCR Peltier Thermal Cycler (MJ Research, USA).

Preparation of protein extract for SDS-PAGE

Arabidopsis seedlings (300 mg fresh weight) were homogenized with small amount of sand and 50 μl of extraction buffer [50 mM *tris*-HCl pH 7.6, 300 mM sucrose, 100 mM NaCl, 10 mM EDTA pH 8.0, 1 mM DTT and 1X Protein inhibitors cocktail (Roche

Diagnostics GmbH Germany)]. After adding 600-µl-extraction buffer, the homogenate was vortexed rapidly and immediately cooled in ice. The crude extract was cleared by two successive centrifugations at 14,000 rpm for 10 min. Protein concentration in the supernatant was measured by the Bradford assay (Bradford 1976), with bovine serum albumin as standard.

Thirty micrograms of total protein extract were separated on 7.5% SDS-polyacrylamide gels and transferred to a nitrocellulose membrane. The western blot was preformed as described above (Blecher et al. 1996).

Antibodies used for Western blot analysis

For ROF1 and ROF2 detection, polyclonal antibodies that have been rised against the recombinant wFKBP73 (α-73) (Blecher et al. 1996; Kurek et al. 1999) diluted 1:3,000 were used. For specific detection of ROF2, immunoaffinity purified specific antibodies against ROF2 were used (detailed below).

A specific ROF2 peptide (amino acid 562–575) was synthesized from the 3′-UTR unconserved region, containing an extra cysteine in its amino-terminus (Genemed Synthesis Inc USA). Two milligram of the ROF2 specific peptide were coupled to a 2 ml SulfoLink gel column (Pierce) according to the manufacturer procedure.

IgG enriched ROF2 peptide antisera (7 ml) was prepared by 50% ammonium sulfate precipitation followed by dialysis against PBS. The ROF2-enriched antiserum was coupled (1 h at room temperature) to the SulfoLink gel column containing the ROF2 peptide. After washing the SulfoLink gel column with PBS, the specific affinity bound antibodies were eluted with glycine buffer (100 mM pH 2.5) and neutralized by adding 100 µl of 1 M *tris*-pH 7.5. The specific ROF2 antibodies were dialyzed against PBS and used for Western blot analysis at a 1:2,000 dilution. For detection of wheat HSP90, the rabbit R2 antiserum against Brassica HSP90 (Krishna et al. 1997) was used.

Labeling with second antibody was preformed by anti rabbit IgG horseradish peroxidase-linked whole antibodies (Pharmacia) diluted 1:15,000. Detection was carried out using ECL Western Blotting Detection Reagents and Analysis System (Amersham Biosciences, UK).

ROF1-wheat HSP90 heterocomplex formation

The ROF1 coding sequence was amplified from 2-week old seedlings cDNA library with specific primers (Table 2), designed with *Bam*HI restriction enzyme for further cloning in expression vectors. The clone was sequenced to confirm lack of mutations.

In order to construct mutated ROF1, a site-directed mutagenesis strategy was applied. Single ROF1 mutation was generated by a PCR reaction using a sense primer, carrying the mutation K484A, with the antisense 3′ ROF1 R primer (Table 2) to amplify a 210 bp fragment at the c-terminal. This fragment was then used as a megaprimer with the 5′ ROF1 F primer to obtain ROF1 K484A. In order to construct a ROF1 TPR domain harboring five mutations, we have further used the ''megaprime'' technique. A primer carrying R488A mutation was used with 3′ ROF1 R primer and the single ROF1 mutation (K484A) clone as a template. The amplified fragment carrying two mutations was then used as reverse megaprimer with forward primer carrying the mutation N454D (Table 2). The amplified fragment was then used as a megaprimer with 5′ ROF1 F primer to obtain full ROF1 harboring three mutations. Five mutations were achieved with forward primer carrying two mutations K404A & N408D (Table 2) and 3′ ROF1 R primer using the ROF1 three mutations clone as a template. The amplified fragment carrying the five mutations was then used as a megaprimer with 5 ROF1 F primer to obtain full ROF1 harboring the five mutations. The ROF1 containing single and five mutations were sequenced to confirm lack of additional mutations.

For expression of ROF1, ROF1 K484A (single mutation), and ROF1 five mutations (K484A, R488A, N454D, K404A, N408D), were cloned into pET28 vector (Novagen) with an amino–terminal His-tagged (Table 1). *Escherichia coli* strain BL21 cells were transformed with the various pET28–ROF1 constructs. For protein expression, single transformed colonies were grown at 37 °C to an OD_{600} and transferred overnight to 4 °C, then diluted 1:25 and grown at 37 °C to an OD_{600}. Induction was performed with 1 mM IPTG for 4 h at 37 °C. Purification conditions of the ROF1 recombinant proteins were according to the manufacturer instructions (Novagen). For adsorption of the purified mutated proteins to Ni-NTA (Novagen) 300 µl ROF1, 400 µl ROF1 K484A mutant and 550 µl ROF1 five mutations were airfuged at 100,000 x g for 15 min with 0.05% Tween-20. The supernatant was rotated for 1 h at 4 °C with 60 µl Ni-NTA resin (50%), washed four times with 1.5 ml of washing buffer (50 mM Pi, 0.3 M NaCl, 20 mM imidazole, 0.05% Tween-20, pH 8.0) and twice with 1.5 ml of incubation buffer (0.1 M Hepes, 10 mM imidazole, 50 mM KCl, pH 7.6). The pellet was incubated for 30 min at 30 °C with 70-µl wheat germ lysate (Promega) supplemented with 10 µg of recombinant human p23 (Harrell et al.

2002) and protease inhibitor cocktail (Complete-Mini, Roche) in the presence or absence of 100 μg pure flag-TPR from rat protein PP5 purified as described in Silverstein et al. (1997). The tubes were shaken every 2 min during the incubation and washed four times with 1.5 ml of washing buffer (as detailed above). The proteins were resolved by a 10% SDS-PAGE followed by Western blotting using the R2 anti-Hsp90 (Krishna et al. 1997) and anti-wFKBP73 (Blecher et al., 1996).

Results

Genome organization and amino acid alignment of ROF1 and ROF2

From the *Arabidopsis* genome database two large FKBPs could be identified: ROF1 and ROF2. ROF1 (3,199 bp) is located on chromosome 3 and ROF2 (3,304 bp) on chromosome 5. Comparison between the genomic structures of ROF1 and ROF2 revealed a high resemblance in the organization of the exons and introns (Fig. 1A). Both genes contain 13 exons of approximately the same length and intron spacing. However, both genes exhibit differences in the first and the last exons. The 5′-UTR of ROF1 (50 bp) is shorter than that of ROF2 (189 bp), while the 3′-UTR of ROF1 (267 bp) is slightly longer than that of ROF2 (203 bp). We assume that the high similarity between the two genes and their organization on the chromosome indicates that ROF1 and ROF2 probably were caused by gene duplication.

Comparison between ROF1 and ROF2 protein sequences with that of the wheat FKBP73, FKBP77, the human FKBP52, and *Arabidopsis* FKBP42 (TWD1) reveals high similarity to the wheat homologues in their amino acid sequences and domain organization (Fig. 1B). ROF1 and ROF2 possess three FKBP12-like domains, whereas, the mammalian homologue hFKBP52 harbors two FKBP12-like domains and the *Arabidopsis* TWD1 only one (Fig. 1B). The first FKBP12-like domain (FKBD1) spans amino acid G-39–D-145 and G-46–R-153 of ROF1 and ROF2, respectively, and possesses the 10 amino acids reported to be essential for binding and maintaining the hydrophobic core of FK506 (van Duyne et al. 1993). The second and third FKBP12-like domains (FKBD2 and FKBD3) span amino acids G-155–K-262 of ROF1 and G-163–K-271 of ROF2 and K-272–K-384 of ROF1, and K-281–K-394 of ROF2, respectively. Sequence comparison between ROF1/ROF2 (85% identity), to the wheat and human FKBPs reveals the highest identity to the wFKBP73 (ROF1 87% and ROF2 84%), lower identity to the wFKBP77 (ROF1 78% and ROF2 80%), 58% with hFKBP52 and only 34% to the TWD1 (Fig. 1B).

ROF1 harbors 3-TPR repeats, which span from K-403 to F-436, N-452 to A-485, and L-486 to K-520. The ROF2-TPR repeats are located between K-413 and F-446, N-462 and A-495, and between M-496 and K-530. The CaMBD (calmodulin binding domain) spans from K-529 to F-545 and from K-539 to L-555 of ROF1 and ROF2, respectively. The amino acids identified as essential for HSP90 binding in the mammalian FKBP52 (Wu et al. 2004) are conserved in the *Arabidopsis* homologues ROF1/ROF2 and TWD1, except for N-408 (Fig. 1B, see asterisks).

Histochemical localization of ROF1 promoter-GUS expression in *Arabidopsis* plants

ROF1-promoter expression in 7-day-old plants

To examine ROF1 expression pattern in planta, we generated *Arabidopsis* transgenic lines expressing the *β*-glucoronidase gene under the control of ROF1 putative promoter (1,848 bp upstream the ATG codon) and analyzed its promoter-GUS activity during developmental stages.

In 7-day-old seedlings, strong expression was observed in the cotyledons, mainly in the vascular system and in (stomata) guard cells, in addition in the shoot apical meristem, hypocotyl-root junction, and in the main root vascular tissue (Fig. 2A). At higher magnification GUS staining was observed in the shoot meristem region, and in the basal cells of the trichomes of primordial leaves (Fig. 2B). The vascular tissue of the primary root, the emerging secondary root (Fig. 2C), and cell elongation zone (Fig. 2A, D) also exhibited GUS staining.

ROF1-promoter expression in 14-and 28-day-old plants

In 14-day-old plants, ROF1-promoter GUS activity was observed in the vascular tissue of the main and lateral roots (Fig. 3A). The expression in lateral root was detected mainly in the root tip and at the root apical meristem (Fig. 3B). In the root tip, GUS staining was observed in the columella (Fig. 3C) and a similar expression pattern was maintained in 28-day-old plants (data not shown).

To determine the expression pattern of ROF1 in root-specific cell layers, transverse sections of 14-and 28–day-old roots were prepared. Strong activity was detected only in the vascular bundle (including the

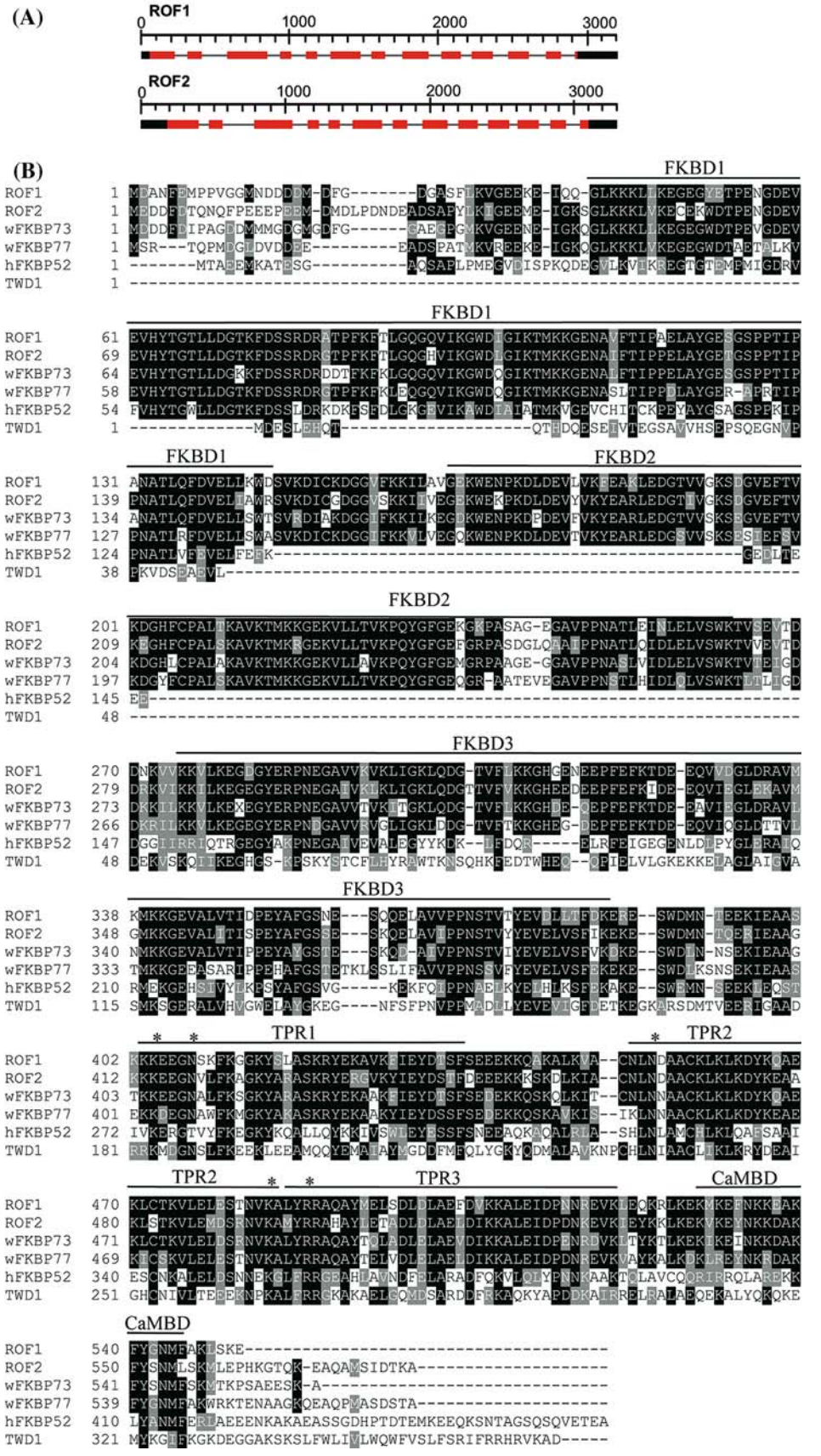

Fig. 1 ROF1 and ROF2 genomic organization and protein alignment. (**A**) Schematic representation of ROF1 and ROF2 genes. Thick-red line specifies the protein coding sequence, thick-black line marks the 5′/3′-UTR and thin black line, the intron region. The sequence was retrieved from TIGR Annotation Version 5 (http://www.tigr.org/tdb/e2k1/ath1/ath1.shtml). (**B**) Amino acid alignment of ROF1 (NP_189160), ROF2 (NP_199668), wFKBP73 (CAA60505), wFKBP77 (CAA68913), hFKBP52 (NP_002005), and TWD1 (NP_188801) *FKBD* FK506 binding domain, *TPR* tetratricopeptide repeats, *CaMBD* calmodulin binding domain. *The amino acids essential for HSP90 binding (in TPR). Sequences were aligned using Clustal W (http://www.ebi.ac.uk/clustalw/) and BoxShade software (http://www.ch.embnet.org/software/BOX_form.html)

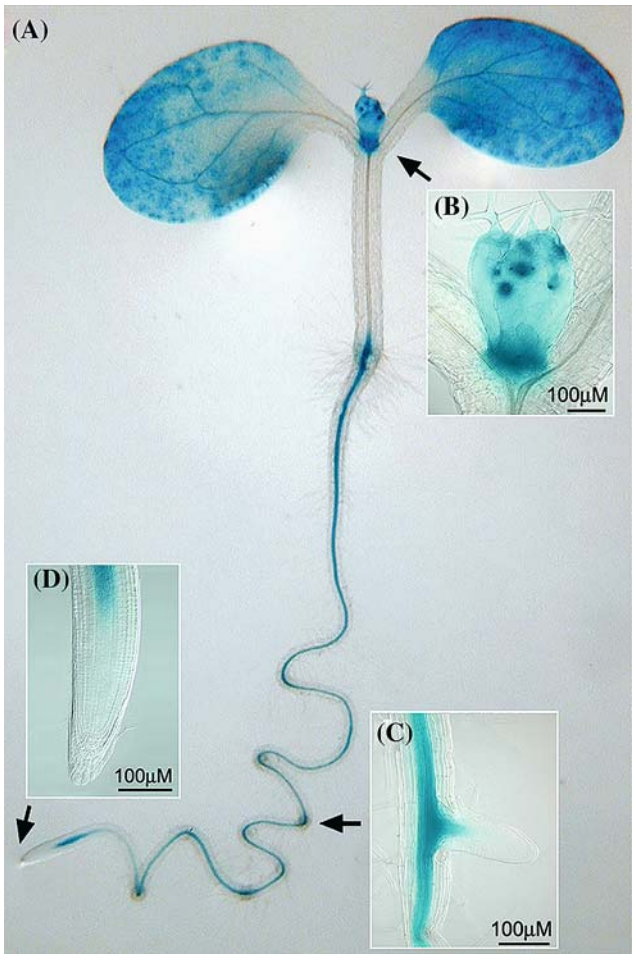

Fig. 2 Histochemical localization of ROF1 promoter-GUS expression in 7-day-old seedlings. Representative expression patterns of ROF1 promoter in whole seedling (**A**), shoot apical meristem and primordial leaves (**B**), emerging lateral root (**C**) and main root (**D**). For GUS staining seedlings were incubated for 2 h

internal stele layer and the pericycle) of the young and mature roots (Fig. 3D, E).

Furthermore, we examined the expression pattern of the ROF1-promoter-GUS cassette during leaf development. In young rosette leaves (second to third true-leaf stage) of 14-day-old seedlings, a basipetal gradient of GUS activity was observed (Fig. 3F). A strong expression was detected in the distal part of the leaf, in hydathodes located in the leaf lobes (Fig. 3F, see arrow), in the stomata (Fig. 3J) and in the basal cells of the trichomes (Fig. 3F see arrow, and 3I). In rosette leaves of 28-day-old plants, ROF1-promoter GUS activity was mainly observed along the vascular tissue and in the hydathodes (Fig. 3G, K). The ROF1 promoter was strongly expressed in the leaf tip and hydathodes (Fig. 3H, see arrows), whereas, GUS expression was barely detected in the center and leaf base of young cauline leaf (from 28-day-old plants). Cauline leaves of secondary young inflorescences showed GUS activity in the leaf tip and in the trichomes basal cells distributed along the leaf (Fig. 3L).

ROF1-promoter expression during flower development

A sequential expression of the ROF1 promoter-GUS cassette was observed during flower development from the sepals to the reproductive organs. ROF1 expression was barely detected in immature flowers and floral buds (up to stage 11 of flower development; Fig. 4A, B). At stage 11, GUS activity was detectable in the upper gynoecium, predominantly in the vascular tissue, and inner wall (Fig. 4C). Increase in expression was observed at stage-12 of flower development in the vascular tissue of sepals and in the style (Fig. 4D), as well as in the ovary inner wall (Fig. 5A). At stage 13, when the bud opens and anthesis occurs, GUS activity was detected in the stamens (Fig. 4E) mainly in the connective tissue (Fig. 5C). At stage 15, a high activity was shown in the anther filament and in the style (Fig. 4F). The increase in ROF1 promoter-driven GUS expression in the style was correlated to the developing vascular tissue (Fig. 5A, B). Closer examination of GUS activity in the anther, showed that it is higher in the connective tissue and anther filament, predominantly in the vascular tissue (Fig. 5C, D). Expression of the ROF1 promoter-GUS construct in pollen grain and petal vascular tissue was observed only after prolonged GUS staining (supplemental Fig. S1). In young siliques (developmental stage 17), expression of GUS was detected in the lower (abscission zone) and upper parts of the silique (Fig. 4G, see insert).

Taken together, ROF1-promoter activity was shown to be developmental and organ specific with highest expression in the vascular elements that are common to all organs analyzed.

ROF1 and ROF2 expression in response to heat stress

ROF1 and ROF2 mRNA expression

In order to obtain further insight into the biological role of ROF2, we have studied the organ specificity and expression levels of ROF1 and ROF2 transcripts in plants grown at 22 °C and after exposure to 37 °C. ROF1 was expressed in all tissues detached from plants grown at 22 °C, whereas ROF2 transcripts were not detectable under the same conditions (Fig. 6). These results are consistent with data describing organ specificity of ROF1 and ROF2 expression profiling at

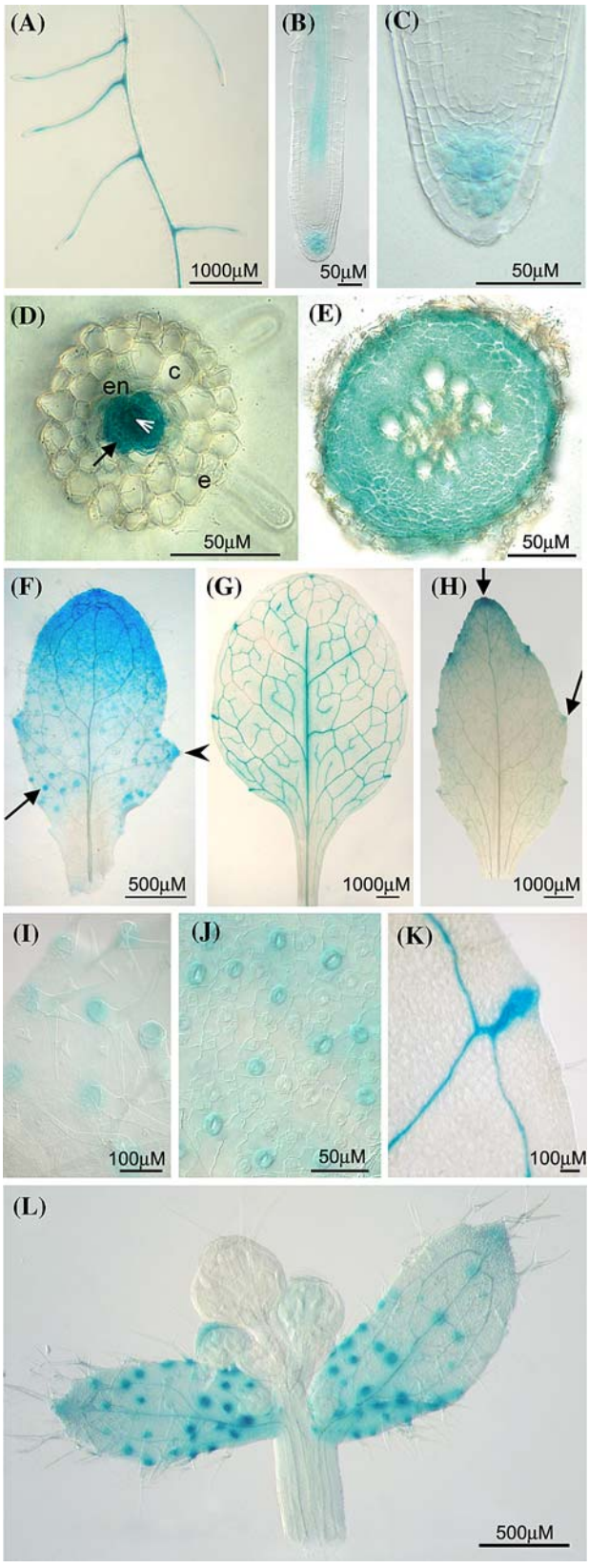

◀ **Fig. 3** Histochemical localization of ROF1 promoter-GUS expression in 14 and 28 days old plants. Representative expression patterns of (A–C) 14-day-old roots. Vascular staining in main and lateral roots (**A**), lateral root staining in elongation zone and root tip (**B**), root tip and apical meristem (**C**). (**D–E**) Transverse sections in specialization zone of 14-day-old (**D**) and 28-day-old soil grown (the outer layers technically cannot be seen in this preparation) (**E**) lateral roots. *e* epidermis, *c* cortex, *en* endodermis. White arrow indicates internal stele layer and black arrow the pericycle. (**F–H**) Rosette leaves from 14-days (**F**) and 28–days-old (**G**) plants, and young cauline leaf of 28–days-old plant (**H**). (**I–K**) Enlargement of the leaf in (**F**), showing basal cells of the trichomes (**I**) and stomata (**J**), and of the leaf in (**G**) showing hydathode and vascular staining (**K**). Cauline leaves of secondary young inflorescence (**L**). For GUS staining roots and leaves were incubated for 20 min (**A–C**, **F**), 30 min (**D**) 2 h (**G**, **H**, **L**) or 3 h (**E**)

physiological conditions, obtained from extensive microarray analysis in the AtGenExpress project (supplemental Fig. S2).

The overall ROF1 GUS-expression results fit well with the microarray data collected from the AtGenExpress project (supplemental Fig. S2). There are few discrepancies, for example, the decline in ROF1 transcript level during flower maturation in the microarray data was not demonstrated in the GUS assays (Fig. 4). This finding could be explained by the fact that data obtained from the promoter analysis (which enables a more detailed examination involving localization of the activity) was compared to the analysis of mRNA expression at steady-state level.

Plants exposed for 1 h to 37 °C, show increased expression of ROF1 mainly in flowers, siliques, and roots, whereas, under the same conditions ROF2 was significantly increased in all organs tested (Fig. 6).

The time course of ROF1 and ROF2 induction at 37 °C and decay at 22 °C was examined by microarray analysis of the AtGenExpress project. Comparison of their expression to that of the classical heat shock protein HSP17.6 class I reveals high similarity of ROF2 to HSP17.6-CI (Wehmeyer et al. 1996). Transcript levels of both ROF1 and ROF2 reached their maximal levels after 1 h exposure to heat stress and remained stable for 3 h at 37 °C (Fig. 7). Estimation of transcript levels shows an increase of about eight fold for ROF1 and 25 fold for ROF2. Decay of the transcript levels was observed after 1 h recovery, attending basal level after 3 h. HSP17.6-CI, showed a similar expression pattern and signal intensity as ROF2 transcript, indicating a possible common regulation pathway.

ROF2-promoter expression in *Arabidopsis*

After we found that ROF2 transcript is induced by heat-stress conditions (Fig. 6), a detailed ROF2

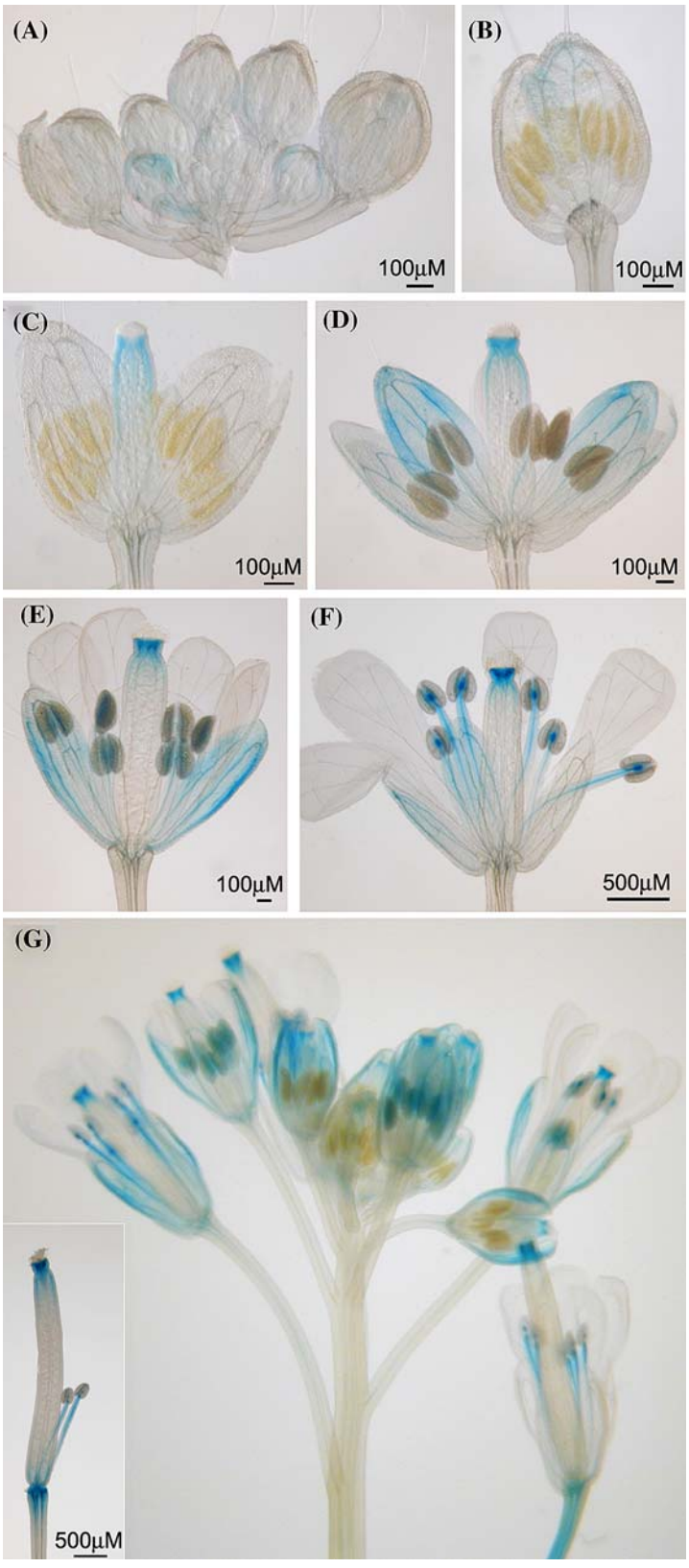

Fig. 4 Histochemical localization of ROF1 promoter-GUS expression during flower development. Representative expression patterns of immature flowers and floral buds (**A**), stages of flower development: 10–11 (**B**), stage 11 (**C**), stage 12 (**D**), stage 13 (**E**), and 15 (**F**). Mature inflorescence containing flowers at various developmental stages (**G**) and a young silique at developmental stage 17 (inset). For GUS staining plants were incubated for 3 h

promoter-GUS analysis was performed on plants after exposure to heat stress (supplemental Fig. S3). The histochemical analysis revealed a pattern similar to that described for ROF1 promoter-GUS activity in plants grown under normal growth conditions. The similarity in expressions is maintained throughout

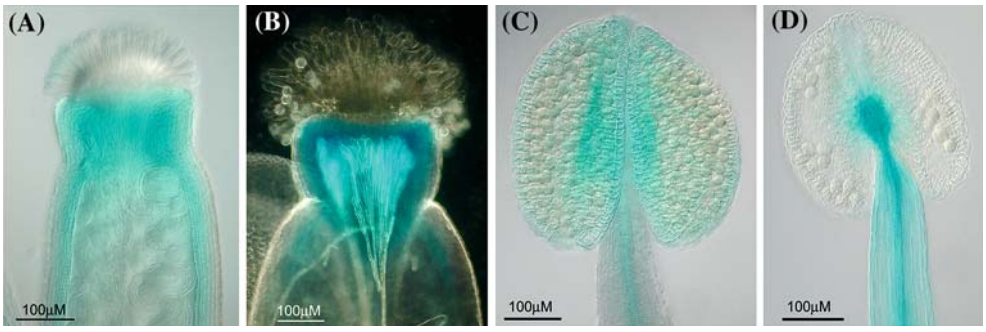

Fig. 5 Expression of ROF1 promoter–GUS in reproductive organs. Stigma and anther of flower at stage 12–13 (**A** and **C**, respectively), and of flower at stage 15 (**B** and **D**, respectively). For GUS staining the relevant parts were incubated for 3 h. Picture (**C**) was photographed by DF (Dark field)

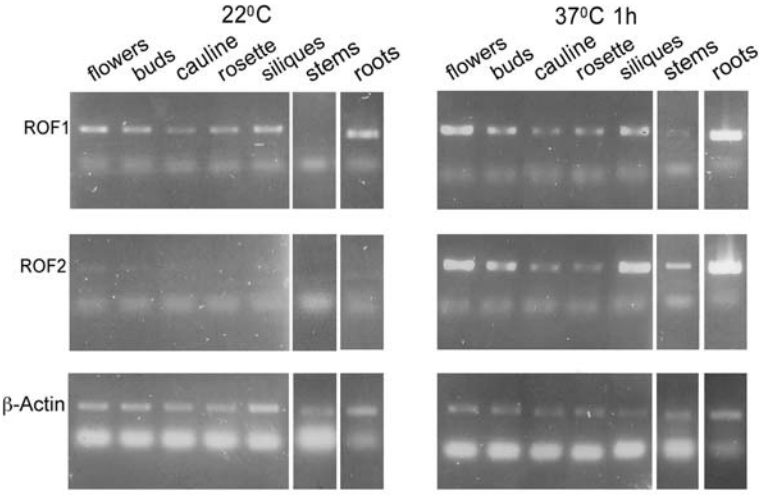

Fig. 6 RT-PCR analysis of ROF1 and ROF2 in organs exposed to heat stress. Total RNA was isolated from various organs and cDNA was synthesized. RT-PCR was preformed using gene specific primers (see Materials and methods Table 2): ROF1 and ROF2 (28 cycles PCR reaction) and β-Actin (24 cycles PCR reaction). The tissues used were from 5–7 weeks old plants, except roots from 2 weeks old MS-grown seedlings. *RT-PCR* reverse transcription polymerase chain reaction

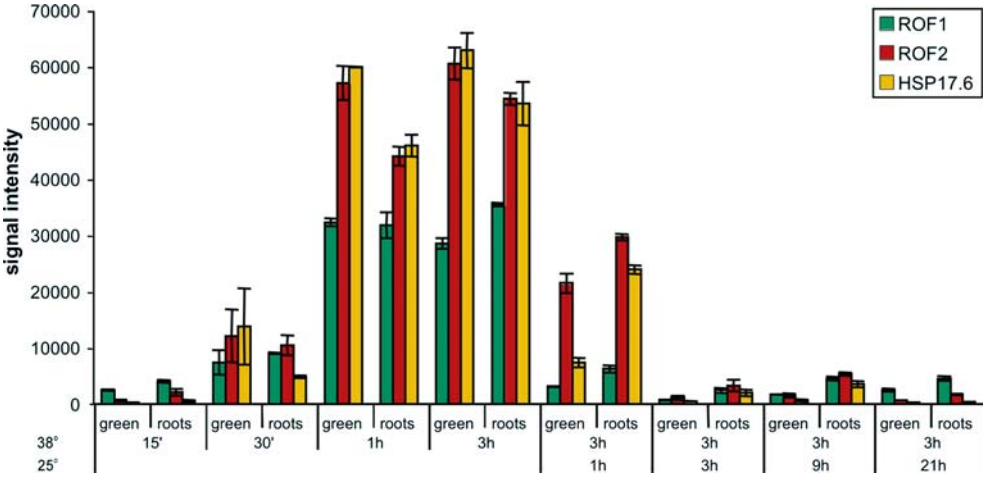

Fig. 7 Induction and decay kinetics of ROF1, ROF2, and HSP 17.6 Class I transcripts. Transcript levels of the indicated genes of 18-day-old seedlings exposed to heat treatment were retrieved from microarray experiments, conducted by the von Koskull-Döring group. Signal values of Affymetrix ATH1 were retrieved using GENEVESTIGATOR (https://www.genevestigator.ethz.ch). Bars indicate standard deviation

plant development: in 7-day-old seedlings, 14-day-old roots, and in flowers at the various developmental stages (supplemental Fig. S3, Figs. 2A, 3A, and 4G, respectively). The comparison of promoter expression analysis of ROF1 and ROF2 GUS fusions did not reveal a difference in the target tissues between the two genes.

Does ROF1 and ROF2 protein accumulation correlate with RNA expression pattern?

To get more indications about the potential function of ROF1 and ROF2 as molecular chaperones, we analyzed their protein levels in response to heat stress. *Arabidopsis* 14-day-old seedlings were exposed to different

heat treatments and each of the two FKBP protein levels were monitored (Fig. 8). In seedlings exposed for 3 h to 37 °C, two proteins were recognized by the α-73. As there are seven large FKBPs in *Arabidopsis* we have confirmed the identity of the higher and lower molecular weight cross reacting proteins as ROF2 and ROF1, respectively (Fig. 8A). The lower molecular weight band (62k Da) was not detected by α-73 in the *rof1*$^-$ mutant protein extracts, while it was present in *rof2*$^-$. This protein was not detected by α-ROF2; hence, it is referred to as ROF1. The higher molecular weight band (65 kDa) was detected by α-73 and α-ROF2 in *rof1*$^-$ extracts but not in *rof2*$^-$ plants, hence it is referred to as ROF2.

To test the temperature dependent ROF1 and ROF2 protein accumulation, seedlings were exposed for 3 h to the temperatures of 22–42 °C. ROF1 was expressed at all temperatures tested except for 42 °C (Fig. 8B, upper panel), whereas, ROF2 was only detectable at 35 °C and 37 °C (Fig. 8B). These results indicate that, in contrast to ROF1, ROF2 protein is strictly heat-stress induced, expressed at a narrow range of elevated temperatures in 14-day-old seedlings. In order to study the stability of the protein after its induction at 37 °C, the seedlings were allowed to recover at 22 °C. Both ROF1 and ROF2 were detectable for at least 4 h of recovery from heat stress (Fig. 8C).

In order understand the inexistence of ROF2 at 42°C in plants exposed directly to this temperature, we have exposed the seedling first to 37 °C and only then exposed them to 42 °C (Fig. 8D). The ROF2 protein, which appeared at 37 °C, remained stable at 42 °C for at least 1.5 h, as compared to plants, which were exposed only to 42 °C for 1.5 h, where no ROF2 could be detected (Fig. 8D). These results indicate that the absence of ROF2 at 42 °C is caused by arrest of its synthesis and is not due to its instability at 42 °C (Fig. 8B, D). The stability of ROF1 depends on the period of exposure to 42 °C: the protein is detectable after 1.5 h (Fig. 8D), whereas, it disappears after 3 h (Fig. 8B, D).

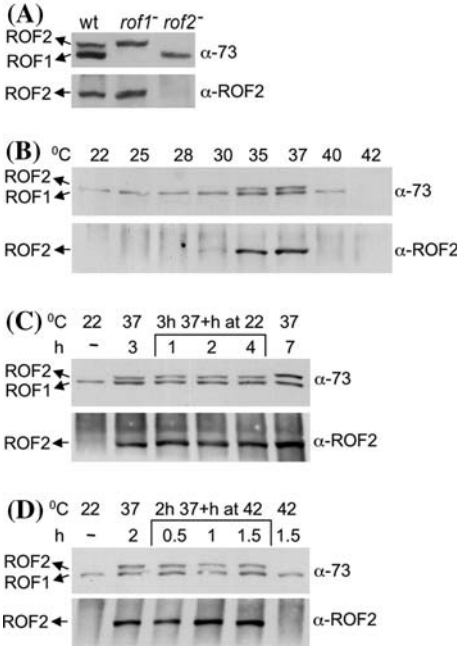

Fig. 8 Expression of ROF1 and ROF2 proteins in seedlings exposed to heat stress. Western blot analysis of total proteins extracted from 14-day-old seedlings. **A** Specificity of polyclonal antibodies against wFKBP73 and ROF2. Protein extracts from wt, *rof1*- and *rof2*-seedlings (see materials and methods) were exposed to 37 °C for 3 h. **B** Temperature dependent expression of ROF1 and ROF2. Seedlings were exposed to 25–42 °C for 3 h. **C** Seedlings were exposed to 37 °C for 3 h, then maintained at 22 °C for the indicated times, or exposed to 37 °C for 7 h. **D** Seedlings were exposed for 2 h to 37 °C followed by 0.5–1.5 h to 42 °C, or directly for 1.5 h to 42 °C. As a control for all treatments the seedlings were grown at 22 °C. Each lane was loaded with 30 μg total proteins. Protein extracts were separated on 7.5% SDS-PAGE and transferred to nitrocellulose membrane. The blots were decorated with anti-wFKBP73 (α-73) (1:3000), or with anti ROF2 specific antibodies (1:2000)

ROF1 binds HSP90: amino acids of the TPR domain, found to be essential for HSP90 binding, are conserved in ROF1

The initial hypothesis that ROF1 may bind HSP90 was reached from the high sequence identity between the TPR region of plant and mammalian large FKBPs (Fig. 1B). In order to find the amino acids relevant for the interaction between ROF1 and HSP90, we took advantage of the crystal structure of mammalian co chaperones possessing TPR such as HOP.

The mammalian HOP protein (Hsp70 and Hsp90 organizing protein) functions as an adaptor protein that provides specific binding sites for Hsp70 and Hsp90 (Chang et al. 1997; Chen and Smith 1998). This protein possesses the TPR-domain and its crystal structure together with its target peptide the HSP90-MEEVD has revealed the amino acids essential for this interaction (K229, N233, N264, K301, and R305) (Scheufler et al. 2000).

To characterize the interaction between ROF1 and HSP90, we performed a HOP-modeled ROF1 comparison, by superimposing the ROF1-TPR domain on the crystal structure of HOP C-terminal TPR domain (TPR2A domain), in complex with the five C-terminal residues of HSP90 (MEEVD peptide) (by using www.expasy.org). ROF1 putative residues involved in binding HSP90 were identified as being: Lys 404; Asn 408; Asn 454;Lys 484; Arg 488 corresponding to the

HOP amino acids which were shown to be essential for HSP90 binding (Fig. 1B, see asterisks).

To examine the contribution of the amino acids defined as being directly involved in binding HSP90, we have produced site directed mutagenised ROF1 protein in the five amino acids.

Recombinant ROF1 proteins carrying mutations were generated in all five amino acids (K404A, N408D, N454D, K484A, R488A) or in a single amino acid (K484A), which was demonstrated to be most important for the interaction (Ward et al. 2002). The mutated proteins were expressed, and heterologous complexes containing HSP90 were obtained in wheat germ lysate (Fig. 9). The resulting complexes were resolved on SDS-PAGE and the presence of the WT or mutated ROF1 and HSP90 were detected by specific antibodies (Fig. 9). Heterocomplexes containing both *Arabidopsis* ROF1 and wheat HSP90 were detected when ROF1 was present (Fig. 9 lane 2) whereas, no complexes were detected in the presence of ROF1 mutated in all the five amino acids (Fig. 9 lane 4) and only traces were detected with the mutated ROF1 K484A protein (Fig. 9 lane 3).

To further validate the interaction between ROF1 and HSP90, competition experiments using the TPR containing rat protein phosphatase 5 (PP5) were performed. The PP5 excluded the binding of the ROF1 to HSP90 as observed in Fig. 9 lanes 6–8.

These results clearly prove the concept that the TPR, and specifically the conserved amino acids found by crystallography of HOP to interact with the HSP90–MEEVD peptide, are conserved in plants, and that the HOP-modeled ROF1-HSP90-MEEVD can serve as an efficient model to predict additional interactions between large FKBPs and HSP90.

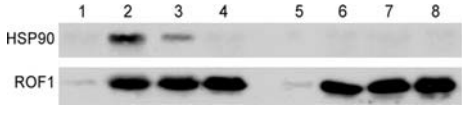

Fig. 9 Heterocomplex formation of ROF1–HSP90 in wheat germ lysate. Lysate from *Escherichia coli* expressing WT ROF1, ROF1 possessing K484A (1 M) or K404A, N408D, N454D, K484A, and R488A (5 M) was adsorbed to Ni-NTA resin and incubated with wheat germ lysate and recombinant human p23, in the absence (lanes 1–4) or presence (lanes 5–8) of Rat PP5 TPR domain. The proteins were resolved on 10% PAGE-SDS followed by Western blotting, and decorated with HSP90 and wFKBP73 antibodies (see materials and methods). Lanes 1 and 5: wheat germ lysate, lanes 2 and 6: WT ROF1, lanes 3 and 7: ROF1 1 M, lanes 4 and 8: ROF1 5 M

Discussion

To get first insights into the function of ROF1 in *Arabidopsis* development we have characterized its temporal and spatial expression pattern by promoter-driven GUS histochemical analysis. ROF1 promoter expression was pronounced in the vascular tissues of roots and leaves of young seedlings and mature plants, in vascular elements of reproductive tissues, such as stigma, the inner wall of the gynoecium's and in the stamens filament (Figs. 2, 3, 4 and 5). Furthermore, strong ROF1 promoter activity was observed in restricted cell types of leaves, namely the basal cells of the trichomes, hydathodes, and stomata (Figs. 2, 3).

A common concept that FKBPs are constitutively expressed has been revised in this study, based on the observation that ROF1and ROF2 expression is developmentally regulated at the organ and tissue levels. Promoter analysis, semi quantitative RT-PCR and data analysis from microarray experiments all strengthen this observation. Previously published data describing a comprehensive analysis of all the immunophilins in *A. thaliana* (He et al. 2004) by semi quantitative RT-PCR indicated that AtFKBP62 (ROF1) and AtFKBP65 (ROF2) transcripts are constitutively expressed (except for roots, expressing low levels of ROF1, or below detection of ROF2). A possibility to explain these discrepancies may be due to technical differences such as usage of more cycles for the PCR reaction by He et al., which we found to minimize the differences between the two genes ROF1 and ROF2.

The pattern of ROF1 and ROF2 expression may point to a potential interaction with known chaperones with a similar expression profile such as HSP90 (Haralampidis al. 2002; Prasinos et al. 2005). The *Arabidopsis* large FKBP TWD1 (Geisler et al. 2003; Perez-Perez et al. 2004) located at the plasma membrane, has been also found to interact with HSP90 via the TPR domain (Kamphausen et al. 2002). However, the other *Arabidopsis* large FKBP, *PAS1* (Vittorioso et al. 1998) although possessing a TPR-domain was not shown to interact with HSP90, but recently shown to interact with a member of the plant-specific family of NAC transcription factors via its C-terminal domain (Smyczynski et al. 2006). *PAS1* was found to be expressed mainly in zones with high levels of mitoic activity such as shoots and root apical meristems (Vittorioso et al., 1998).

In contrast to the dramatic developmental phenotypes of *twd1* and *PAS1* knockout mutants, the *Arabidopsis rof1* and *rof2* mutants (Fig. 8A) have not shown clear phenotypes under normal growth conditions. We suggest

that although ROF1 is present at 22 °C, its function may appear mainly after exposure to heat stress. At this condition, its close homologue ROF2 could compensate and hence no phenotype was observed. Therefore the recently obtained *rof1*/*rof2* double-mutants and the single *rof1, rof2* mutants are currently tested for phenotype after exposure to various heat-stress treatments. It should be mentioned that while ROF1 and ROF2 are close homologues, which may compensate for each other, *twd1* and *PAS1* are unique in their structure and therefore their phenotypes were possibly easier to detect.

The ROF2 characterized in this study was shown to be a bona fide heat-stress gene. At regular growth condition of 22 °C, ROF2 transcript level was below detection limit, whereas, it was highly expressed in response to heat (37 °C) in all plant tissues tested. The kinetics of the induction and decay, as well as the amounts of ROF2 transcript, were similar to those observed during heat induction for the small heat-shock protein HSP17.6 Class I (HSP17.6-CI) (Wehmeyer et al. 1996; Lohmann et al. 2004).

ROF2 expression was down regulated in mutants defective in heat shock transcription factors (*AthsfA1a*/*AthsfA1b*) similarly to major heat shock proteins such as HSP17.6-CI, HSP101, HSP70, and HSP83.1. In these mutants, the ROF2 displayed the most dramatic markdown (Busch et al. 2005). These results point to the possibility that one or both of the *Arabidopsis* heat-stress transcription factors HsfA1a and Hsf A1b may regulate the expression of ROF2.

Comparison between ROF1 and ROF2 protein accumulation patterns shows that only ROF1 is detected at 22 °C. Differential accumulation between the two ROF proteins was also observed at 42 °C, a temperature in which the ROF1 protein is accumulated, while the ROF2 protein is absent. We interpret this result by the arrest of ROF2 synthesis rather than instability of the protein at this temperature (Fig. 8D).

We have shown that ROF1 binds HSP90, the interaction is specific, and thus ROF1 is a novel HSP90 client protein. The ROF1-HSP90 interaction occurs via the TPR domain in which 5-amino acid-key residues were found to be essential for this interaction (Fig. 9). Using the mammalian HOP (HSP70 and HSP90 organizing protein) crystal structure we have modeled the ROF1 TPR structure. We have identified the amino acids responsible for interaction with HSP90. These amino acids were site directed mutagenized followed by binding assay analysis, which validated our concept of conservation of these amino acids, which are responsible for the interaction between the large FKBPs and HSP90 (Ward et al. 2002; Scheufler et al. 2000; Wu et al. 2004; Sinars et al. 2003).

The expression pattern of ROF1 and ROF2 described in this study shows high resemblance to the pattern of expression of the *Arabidopsis* HSP90 (Haralampidis et al. 2002; Prasinos et al. 2005). When comparing the reported promoter expression profile of *Arabidopsis* AtHSP90-3 (At5g56030.1) and AtHSP90-1 (At5g52640.1), we observed a similar pattern between AtHSP90-3 with that of ROF1. For example, both ROF1 and HSP90-3 are highly expressed in bundles of the siliques, roots meristems and vascular system. The expression pattern of ROF2 resembles that of AtHSP90-1, both being detected only after heat stress (Haralampidis et al. 2002; Prasinos et al. 2005).

The AtHSP90-3 and ROF1 promoters harbor common sequences known to mediate heat shock and other-stress stimuli. For example both contain heat-stress elements (HSEs, elements for binding heat shock transcription factor) (Wu 1995) at about -200 bp and CCAAT sequences essential for binding the C/EBP transcription factors (Akira et al. 1990), which acts cooperatively with HSEs (Prasinos et al. 2005). The ROF2, as the AtHSP90-1 promoter contains HSEs and STREs (Stress Response elements), involved in general stress response (Haralampidis et al. 2002).

In conclusion, our biochemical assays, showing interaction between the ROF1 and HSP90, together with the spatial expression pattern and induction by similar stresses of the ROF1/2 and AtHSP90-3/HSP90-1 lead us to the hypothesis that these proteins complexes are formed and function in vivo. For example, the ROF1-AtHSP90-3 may function under regular growth conditions as well as after heat stress, whereas the ROF2-AtHSP90-1 under heat-stress conditions.

HSP90 is known to have a diverse set of client proteins and participate in various developmentally, hormonally, and morphogenetically regulated processes (Queitsch et al. 2002; Sangster and Queitsch 2005). We suggest that part of the multiple functions of HSP90 can be attributed to the specific interactions between HSP90 and either ROF1 or ROF2.

In spite of the similarity between ROF1 and ROF2, their expression patterns emerge to be differentially regulated as shown during heat-stress response.

We propose that the *Arabidopsis* ROF1 and ROF2 large FKBPs function in concert with specific HSP90 partners and contribute to plant growth and response to environmental factors.

Acknowledgment This work was supported by a grant from the Israeli National Academy of Science to A. Breiman; by CONICET–PIP6167 and ANPCyT PICT2003/01–14123 to M. Galigniana; by FEBS short-term fellowship to K. Aviezer-Hagai. We thank Dedi Meiri for his generous contribution and fruitful discussions. We also thank Neomi Dafni for her technical help.

References

Akira S, Isshiki H, Sugita T, Tanabe O, Kinoshita S, Nishio Y, Nakajima T, Hirano T, Kishimoto T (1990) A nuclear factor for IL-6 expression (NF-IL6) is a member of a C/EBP family. Embo J 9:1897–1906

Bechtold N, Ellis J, Pelletier G (1993) In planta *Agrobacterium*-mediated gene transfer by infiltration of adult *Arabidopsis thaliana* plants. CR Acad Sci Paris 316:1194–1199

Blecher O, Erel N, Callebaut I, Aviezer K, Breiman A (1996) A novel plant peptidyl-prolyl-*cis-trans*-isomerase (PPIase): cDNA cloning, structural analysis, enzymatic activity and expression. Plant Mol Biol 32:493–504

Bowman J (1994) Arabidopsis: an atlas of morphology and development. Springer, New York

Bradford MM (1976) A rapid and sensitive method for the quantitation of microgram quantities of protein utilizing the principle of protein-dye binding. Anal Biochem 72:248–254

Breiman A, Fawcett TW, Ghirardi ML, Mattoo AK (1992) Plant organelles contain distinct peptidylprolyl *cis,trans*-isomerases. J Biol Chem 267:21293–21296

Busch W, Wunderlich M, Schoffl F (2005) Identification of novel heat shock factor-dependent genes and biochemical pathways in *Arabidopsis thaliana*. Plant J 41:1–14

Carrigan PE, Sikkink LA, Smith DF, Ramirez-Alvarado M (2006) Domain:domain interactions within Hop, the Hsp70/Hsp90 organizing protein, are required for protein stability and structure. Protein Sci 15:522–532

Chambraud B, Rouviere-Fourmy N, Radanyi C, Hsiao K, Peattie DA, Livingston DJ, Baulieu EE (1993) Overexpression of p59-HBI (FKBP59), full length and domains, and characterization of PPlase activity. Biochem Biophys Res Commun 196:160–166

Chang HC, Nathan DF, Lindquist S (1997) In vivo analysis of the Hsp90 cochaperone Sti1 (p60). Mol Cell Biol 17:318–325

Chen S, Smith DF (1998) Hop as an adaptor in the heat shock protein 70 (Hsp70) and hsp90 chaperone machinery. J Biol Chem 273:35194–35200

Christou P, Ford TL. (1995) The impact of selection parameters on the phenotype and genotype of transgenic rice callus and plants. Transgenic Res 4:44–51

Clark MS (1997) Plant molecular biology: a laboratory manual. Springer-Verlag, Berlin Heidelberg, pp 8–9

Clough SJ, Bent AF (1998) Floral dip: a simplified method for *Agrobacterium*-mediated transformation of *Arabidopsis thaliana*. Plant J 16:735–743

Das AK, Cohen PW, Barford D (1998) The structure of the tetratricopeptide repeats of protein phosphatase 5: implications for TPR-mediated protein-protein interactions. Embo J 17:1192–1199

Davies TH, Ning YM, Sanchez ER (2005) Differential control of glucocorticoid receptor hormone-binding function by tetratricopeptide repeat (TPR) proteins and the immunosuppressive ligand FK506. Biochemistry 44:2030–2038

Dornan J, Taylor P, Walkinshaw MD (2003) Structures of immunophilins and their ligand complexes. Curr Top Med Chem 3:1392–1409

Dwivedi RS, Breiman A, Herman EM (2003) Differential distribution of the cognate and heat-stress-induced isoforms of high Mr *cis-trans*-prolyl peptidyl isomerase (FKBP) in the cytoplasm and nucleoplasm. J Exp Bot 54:2679–2689

Eckhoff A, Granzin J, Kamphausen T, Buldt G, Schulz B, Weiergraber OH (2005) Crystallization and preliminary X-ray analysis of immunophilin-like FKBP42 from *Arabidopsis thaliana*. Acta Crystallograph Sect F Struct Biol Cryst Commun 61:363–365

Fanghanel J, Fischer G (2004) Insights into the catalytic mechanism of peptidyl prolyl *cis*/*trans* isomerases. Front Biosci 9:3453–3478

Faure JD, Gingerich D, Howell SH (1998a) An *Arabidopsis* immunophilin, AtFKBP12, binds to AtFIP37 (FKBP interacting protein) in an interaction that is disrupted by FK506. Plant J 15:783–789

Faure JD, Vittorioso P, Santoni V, Fraisier V, Prinsen E, Barlier I, Onckelen HV, Caboche M, Bellini C (1998b) The *PASTICCINO* genes of *Arabidopsis thaliana* are involved in the control of cell division and differentiation. Development 125:909–918

Fire A, Xu S, Montgomery MK, Kostas SA, Driver SE, Mello CC (1998) Potent and specific genetic interference by double-stranded RNA in Caenorhabditis elegans. Nature 391:806–811

Fischer G, Tradler T, Zarnt T (1998) The mode of action of peptidyl prolyl *cis*/*trans* isomerases in vivo: binding vs. catalysis. FEBS Lett 426:17–20

Galat A (2004) A note on clustering the functionally-related paralogues and orthologues of proteins: a case of the FK506-binding proteins (FKBPs). Comput Biol Chem 28:129–140

Galat A (2003) Peptidylprolyl *cis*/*trans* isomerases (immunophilins): biological diversity–targets–functions. Curr Top Med Chem 3:1315–1347

Geisler M, Girin M, Brandt S, Vincenzetti V, Plaza S, Paris N, Kobae Y, Maeshima M, Billion K, Kolukisaoglu UH, Schulz B, Martinoia E (2004) *Arabidopsis* immunophilin-like TWD1 functionally interacts with vacuolar ABC transporters. Mol Biol Cell 15:3393–3405

Geisler M, Kolukisaoglu HU, Bouchard R, Billion K, Berger J, Saal B, Frangne N, Koncz-Kalman Z, Koncz C, Dudler R, Blakeslee JJ, Murphy AS, Martinoia E, Schulz B (2003) TWISTED DWARF1, a unique plasma membrane-anchored immunophilin-like protein, interacts with *Arabidopsis* multidrug resistance-like transporters AtPGP1 and AtPGP19. Mol Biol Cell 14:4238–4249

Gleave AP (1992) A versatile binary vector system with a T-DNA organisational structure conducive to efficient integration of cloned DNA into the plant genome. Plant Mol Biol 20:1203–1207

Goebl M, Yanagida M (1991) The TPR snap helix: a novel protein repeat motif from mitosis to transcription. Trends Biochem Sci 16:173–177

Haralampidis K, Milioni D, Rigas S, Hatzopoulos P (2002) Combinatorial interaction of *cis* elements specifies the expression of the *Arabidopsis* AtHsp90-1 gene. Plant Physiol 129:1138–1149

Harrar Y, Bellec Y, Bellini C, Faure JD (2003) Hormonal control of cell proliferation requires PASTICCINO genes. Plant Physiol 132:1217–1227

Harrell JM, Kurek I, Breiman A, Radanyi C, Renoir JM, Pratt WB, Galigniana MD (2002) All of the protein interactions that link steroid receptor.hsp90.immunophilin heterocomplexes to cytoplasmic dynein are common to plant and animal cells. Biochemistry 41:5581–5587

He Z, Li L, Luan S (2004) Immunophilins and parvulins. Superfamily of peptidyl prolyl isomerases in *Arabidopsis*. Plant Physiol 134:1248–1267

Hueros G, Rahfeld J, Salamini F, Thompson R (1998) A maize FK506-sensitive immunophilin, mzFKBP-66, is a peptidylproline *cis-trans*-isomerase that interacts with calmodulin and a 36-kDa cytoplasmic protein. Planta 205:121–131

Jefferson RA, Kavanagh TA, Bevan MW (1987) GUS fusions: beta-glucuronidase as a sensitive and versatile gene fusion marker in higher plants. Embo J 6:3901–3907

Jin YJ, Burakoff SJ, Bierer BE (1992) Molecular cloning of a 25-kDa high affinity rapamycin binding protein, FKBP25. J Biol Chem 267:10942–10945

Kamphausen T, Fanghanel J, Neumann D, Schulz B, Rahfeld JU (2002) Characterization of *Arabidopsis thaliana* AtFKBP42 that is membrane-bound and interacts with Hsp90. Plant J 32:263–276

Krishna P, Reddy RK, Sacco M, Frappier JR, Felsheim RF (1997) Analysis of the native forms of the 90 kDa heat shock protein (hsp90) in plant cytosolic extracts. Plant Mol Biol 33:457–466

Kurek I, Aviezer K, Erel N, Herman E, Breiman A (1999) The wheat peptidyl prolyl *cis-trans*-isomerase FKBP77 is heat induced and developmentally regulated. Plant Physiol 119:693–704

Lohmann C, Eggers-Schumacher G, Wunderlich M, Schoffl F (2004) Two different heat shock transcription factors regulate immediate early expression of stress genes in *Arabidopsis*. Mol Genet Genomics 271:11–21

Luan S, Kudla J, Gruissem W, Schreiber SL (1996) Molecular characterization of a FKBP-type immunophilin from higher plants. Proc Natl Acad Sci USA 93:6964–6969

Luan S, Lane WS, Schreiber SL (1994) pCyP B: a chloroplast-localized, heat shock-responsive cyclophilin from fava bean. Plant Cell 6:885–892

Magiri EN, Farchi-Pisanty O, Avni A, Breiman A (2006) The expression of the large rice FK506 binding proteins (FKBPs) demonstrate tissue specificity and heat stress responsiveness. Plant Sci 170:695–704

Owens-Grillo JK, Stancato LF, Hoffmann K, Pratt WB, Krishna P (1996) Binding of immunophilins to the 90 kDa heat shock protein (hsp90) via a tetratricopeptide repeat domain is a conserved protein interaction in plants. Biochemistry 35:15249–15255

Perez-Perez JM, Ponce MR, Micol JL (2004) The ULTRACURVATA2 gene of *Arabidopsis* encodes an FK506-binding protein involved in auxin and brassinosteroid signaling. Plant Physiol 134:101–117

Pirkl F, Buchner J (2001) Functional analysis of the Hsp90-associated human peptidyl prolyl *cis*/*trans* isomerases FKBP51, FKBP52 and Cyp40. J Mol Biol 308:795–806

Prasinos C, Krampis K, Samakovli D, Hatzopoulos P (2005) Tight regulation of expression of two *Arabidopsis* cytosolic Hsp90 genes during embryo development. J Exp Bot 56:633–644

Pratt WB, Galigniana MD, Harrell JM, DeFranco DB (2004) Role of hsp90 and the hsp90-binding immunophilins in signalling protein movement. Cell Signal 16:857–872

Queitsch C, Sangster TA, Lindquist S (2002) Hsp90 as a capacitor of phenotypic variation. Nature 417:618–624

Reddy RK, Kurek I, Silverstein AM, Chinkers M, Breiman A, Krishna P (1998) High-molecular-weight FK506-binding proteins are components of heat-shock protein 90 heterocomplexes in wheat germ lysate. Plant Physiol 118:1395–1401

Riggs DL, Roberts PJ, Chirillo SC, Cheung-Flynn J, Prapapanich V, Ratajczak T, Gaber R, Picard D, Smith DF (2003) The Hsp90-binding peptidylprolyl isomerase FKBP52 potentiates glucocorticoid signaling in vivo. Embo J 22:1158–1167

Romano P, Gray J, Horton P, Luan S (2005) Plant immunophilins: functional versatility beyond protein maturation. New Phytol 166:753–769

Sanchez ER, Faber LE, Henzel WJ, Pratt WB (1990) The 56–59-kilodalton protein identified in untransformed steroid receptor complexes is a unique protein that exists in cytosol in a complex with both the 70- and 90-kilodalton heat shock proteins. Biochemistry 29:5145–5152

Sangster TA, Queitsch C (2005) The HSP90 chaperone complex, an emerging force in plant development and phenotypic plasticity. Curr Opin Plant Biol 8:86–92

Scheufler C, Brinker A, Bourenkov G, Pegoraro S, Moroder L, Bartunik H, Hartl FU, Moarefi I (2000) Structure of TPR domain-peptide complexes: critical elements in the assembly of the Hsp70–Hsp90 multichaperone machine. Cell 101:199–210

Schreiber SL (1991) Chemistry and biology of the immunophilins and their immunosuppressive ligands. Science 251:283–287

Silverstein AM, Galigniana MD, Chen MS, Owens-Grillo JK, Chinkers M, Pratt WB (1997) Protein phosphatase 5 is a major component of glucocorticoid receptor.hsp90 complexes with properties of an FK506-binding immunophilin. J Biol Chem 272:16224–16230

Sinars CR, Cheung-Flynn J, Rimerman RA, Scammell JG, Smith DF, Clardy J (2003) Structure of the large FK506-binding protein FKBP51, an Hsp90-binding protein and a component of steroid receptor complexes. Proc Natl Acad Sci USA 100:868–873

Smith DF, Baggenstoss BA, Marion TN, Rimerman RA (1993) Two FKBP-related proteins are associated with progesterone receptor complexes. J Biol Chem 268:18365–18371

Smyczynski C, Roudier F, Gissot L, Vaillant E, Grandjean O, Morin H, Masson T, Bellec Y, Geelen D, Faure JD (2006) The C-terminus of the immunophilin PASTICCINO1 is required for plant development and for interaction with a NAC-like transcription factor. J Biol Chem

Smyth DR, Bowman JL, Meyerowitz EM (1990) Early flower development in *Arabidopsis*. Plant Cell 2:755–767

Standaert RF, Galat A, Verdine GL, Schreiber SL (1990) Molecular cloning and overexpression of the human FK506-binding protein FKBP. Nature 346:671–674

Van Duyne GD, Standaert RF, Karplus PA, Schreiber SL, Clardy J (1993) Atomic structures of the human immunophilin FKBP-12 complexes with FK506 and rapamycin. J Mol Biol 229:105–124

Vittorioso P, Cowling R, Faure JD, Caboche M, Bellini C (1998) Mutation in the *Arabidopsis* PASTICCINO1 gene, which encodes a new FK506-binding protein-like protein, has a dramatic effect on plant development. Mol Cell Biol 18:3034–3043

Vucich VA, Gasser CS (1996) Novel structure of a high molecular weight FK506 binding protein from *Arabidopsis thaliana*. Mol Gen Genet 252:510–517

Ward BK, Allan RK, Mok D, Temple SE, Taylor P, Dornan J, Mark PJ, Shaw DJ, Kumar P, Walkinshaw MD, Ratajczak T (2002) A structure-based mutational analysis of cyclophilin 40 identifies key residues in the core tetratricopeptide repeat domain that mediate binding to Hsp90. J Biol Chem 277:40799–40809

Wehmeyer N, Hernandez LD, Finkelstein RR, Vierling E (1996) Synthesis of small heat-shock proteins is part of the developmental program of late seed maturation. Plant Physiol 112:747–757

Weiergraber OH, Eckhoff A, Granzin J (2006) Crystal structure of a plant immunophilin domain involved in regulation of MDR-type ABC transporters. FEBS Lett 580:251–255

Wesley SV, Helliwell CA, Smith NA, Wang MB, Rouse DT, Liu Q, Gooding PS, Singh SP, Abbott D, Stoutjesdijk PA, Robinson SP, Gleave AP, Green AG, Waterhouse PM (2001) Construct design for efficient, effective and high-throughput gene silencing in plants. Plant J 27:581–590

Wu B, Li P, Liu Y, Lou Z, Ding Y, Shu C, Ye S, Bartlam M, Shen B, Rao Z (2004) 3D structure of human FK506-binding protein 52: implications for the assembly of the glucocorticoid receptor/Hsp90/immunophilin heterocomplex. Proc Natl Acad Sci USA 101:8348–8353

Wu B, Li P, Shu C, Shen B, Rao Z (2003) Crystallization and preliminary crystallographic studies of the C-terminal domain of human FKBP52. Acta Crystallogr D Biol Crystallogr 59:2269–2271

Wu C (1995) Heat shock transcription factors: structure and regulation. Annu Rev Cell Dev Biol 11:441–469

Zhang X, Wang Y, Li H, Zhang W, Wu D, Mi H (2004) The mouse FKBP23 binds to BiP in ER and the binding of C-terminal domain is interrelated with Ca^{2+} concentration. FEBS Lett 559:57–60

Zimmermann P, Hennig L, Gruissem W (2005) Gene-expression analysis and network discovery using Genevestigator. Trends Plant Sci 10:407–409

Zimmermann P, Hirsch-Hoffmann M, Hennig L, Gruissem W (2004) GENEVESTIGATOR. *Arabidopsis* microarray database and analysis toolbox. Plant Physiol 136:2621–2632